

Theoretical study of structural and optical properties of ZnO in wurtzite phase

Y. Benkrima ^{a*}, S. Benhamida ^b, D. Belfennache ^c

^a *Department of Exact Sciences, ENS Ouargla, Algeria.*

^b *Laboratory of Radiation, Plasma and Surface Physics (LRPPS), Faculty of Mathematics and Material Sciences, Kasdi Merbah Ouargla University, Route de Ghardaia, BP n°511, Ouargla 30000 (Algeria).*

^c *Research Center in Industrial Technologies CRTI, P.O. Box 64, Cheraga, 16014 Algiers, Algeria.*

Our calculations are done with the help of density functional theory (DFT). Actually, we could find the structural and optical properties of the wurtzite-type ZnO compound. The pseudo-potential linearised augmented plane wave (PP-LAPW) method is applied to solve the Kohn-Sham equations. The results are obtained using Both Generalized Gradient Approximation according to the scheme described by Perdew-Burke-Ernzerhof (GGA-PBE) and Local Density Approximation according to the scheme described by Ceperly-Alder (LDA-CA) approximations as two types of exchange-correlation. The convergence of energy and charge has been checked. This is in order to study the properties of the ground state. It was found that the primary cell constants calculated in the equilibrium state are very close to the previous theoretical works. The general results of optical properties including the imaginary part of the dielectric constant, reflectivity, absorption coefficient, refractive index, optical conductivity, and extinction coefficient of wurtzite-phase ZnO under the imposed conditions are discussed and compared with previous works. Our results show new and important optical properties. Besides, we predicted the behavior of transparent conductive oxides in the direction of light.

(Received October 1, 2022; Accepted January 7, 2023)

Keywords: ZnO, Structural properties, Reflectivity, Absorption, Refractive index, Optical conductivity.

1. Introduction

Zinc Oxide (ZnO) is classified among the semiconductors that have a wide and direct energy gap of about (3.4eV), and a very large exciton energy of about (60 megavolts) [1]. In recent years, many researchers have been interested in studying semiconductor-type compounds such as ZnO, due to its advantages and properties that allow it to take the lead in the formation of compounds with industrial and technological uses where ZnO has diverse applications, for example: gas sensors, catalysts, electronic and optoelectronic devices [2-5]. However, according to the literatures [6,7] in ordinary conditions, the dynamically stable phase is the (B4) wurtzite phase, which has a tetrahedral surface, and also has a covalent bonding of the Sp³ type. Several studies have been conducted to investigate the optical properties of the wurtzite phase ZnO [8,9]. John et al. [10] presented a theoretical study on the structural, electronic and optical properties of ZnO wurtzite, by using the Full Potential Linearized Augmented Plane Wave (FP-LAPW) method is applied to solve the Kohn-Sham equations. Other researchers have also studied the use of LDA and PW92 approximations as well as the linear and non-linear optical response of ZnO using the ABINIT code [11]. In addition, a specific explanation of the electronic and optical properties of BN (Bk) phase ZnO under pressure has been calculated using CASTEP program with a GGA+U method by Wang et al [12]. Not to mention the numerous studies that are based on finding optical properties in several conditions and using different codes [13-16].

* Corresponding author: benkrimayamina1@gmail.com

<https://doi.org/10.15251/DJNB.2023.181.11>

This paper is focus on the study of structural parameters, electronic and both optical coefficients, imaginary and real constant of optical properties with siesta code within the DFT theory. Theremain paper is organized as follow; section 2 exposed the detail of calculations then the results with the discussions in section 3 and in the end the conclusion.

2. Materials and methods

ZnO wurtzite is utilized in underlying and electronic property computations. To get solid outcomes, a profoundly exact Pseudo Potential Linearized Augmented Plane Wave (PP-LAPW) strategy is used, as carried out in the Siesta program using DFT. The relation impact is dealt with utilizing the LDA [17] and the PBE-GGA. We utilized in these study two essential boundaries, for example, the cutoff active energy for 350 eV plane waves and a $3 \times 3 \times 3$ k-point network utilizing the Monkhorst-Pack technique. The intense energy of the particles gathered together and entered the region under 5×10^{-5} eV/atom, and the Hellman Feynman ionic strength of particles in this region was under 0.05 eV/Å. To acquire more precise outcomes for all electronic and optical properties, we expanded the quantity of k-points to $3 \times 3 \times 6$.

3. Results and Discussion

3.1. Structural Properties

We used the DFT and the Siesta program in order to calculate the primary cell constants. We found the following values: 3.284 Å for the constant a, and the value 5.339 Å for the constant c. Since it is a hexagonal structure, we find we find $a=b$. The angle constants $\alpha = \beta = 90.042^\circ$ and $\gamma = 120.242^\circ$. In this work, we also calculated μ , which is the internal variable that determines the length of the bond between zinc and oxygen, we got the value estimated at 0.7918.

It is clear from the table that the results we obtained correspond with the theoretical and experimental results mentioned above, as in works [18-29]. We also calculated the percentage of error in the obtained values, in order to compare them to the experimental values taken as a reference. We found the error value for the constant a 1.07% and for the constant c 1.9%. We notice that these calculated error values are very small, which indicates that the calculation method is very accurate.

Table1.comparison of primary cell constants of ZnO with theoretical and experimental results.

The used method	a (Å)	c (Å)	c/a	μ (Å)
Our results in GGA	3.284	5.339	1.6257	0.7918
GGA-PBE [18]	3.288	5.305	1.6134	0.7878
GGA-PBE [19]	3.286	5.299	1.6125	0.7875
GGA-PBE [20]	3.282	5.294	1.6130	0.7876
LDA [21]	3.186	5.150	1.6164	0.7888
Experimental work [22]	3.250	5.207	1.6021	0.7804
Experimental work [23]	3.242	5.188	1.6002	0.7834
Experimental work [24]	3.250	5.210	1.6030	0.7843
GGA-PBE [25]	3.289	5.308	1.6138	0.7879
LDA [26]	3.250	5.210	1.6030	0.7843
LDA [27]	3.189	5.237	1.6534	0.7974
Experimental work [28]	3.250	5.204	1.6020	0.3820
Experimental work [29]	3.258	5.201	1.6010	0.3823

3.2. Optical properties

Ab Initio Calculations on Structural electronic and Optical Properties of ZnO in wurtzite Phase It is important to resort to optical properties in order to understand the nature of material and

its usage in opto-electronic devices. We know that the interaction of photons with the electrons can be described regarding time-dependent perturbations of the ground-state electronic states. Transitions between occupied and unoccupied states are caused due to the electric field of the photon. To some extent, the resulting spectra can be defined as a joint density of States between conduction bands and valence. The following function $\varepsilon(\omega)$ can serve to describe the optical response of a material to the electromagnetic field at all energy levels:

$$\varepsilon(\omega) = \varepsilon_1(\omega) + i\varepsilon_2(\omega) \quad (1)$$

where $\varepsilon_1(\omega)$ and $\varepsilon_2(\omega)$: real and imaginary part of the dielectric function.

Real part of the dielectric function $\varepsilon_1(\omega)$ mentions to the dispersion of the incident photons by the material, while the imaginary part $\varepsilon_2(\omega)$ means the energy absorbed by the material. There are two (2) contributions to complex dielectric function $\varepsilon(\omega)$: intraband and interband transitions. The first contribution is dominant only for metals. The second one can be further separated into direct and indirect transitions. The indirect interband transitions are deserted here. They contain scattering the phonon and are expected to give small contributions to the dielectric function [11, 30]. The imaginary part $\varepsilon_2(\omega)$ is calculated based on the contribution of the direct interband transitions from the occupied to unoccupied states, and the calculation is associated with the energy eigenvalue and energy wave functions. Concerning the real part $\varepsilon_1(\omega)$, it can be found from its corresponding $\varepsilon_2(\omega)$ by Kramers-Kronig transformation in the form [31].

$$\varepsilon_1(\omega) = 1 + \frac{2}{\pi} P \int_0^{\infty} \frac{\omega' \varepsilon_2(\omega') d\omega'}{\omega'^2 - \omega^2} \quad (2)$$

where P is principle value of the integral.

By knowing the $\varepsilon_1(\omega)$ and $\varepsilon_2(\omega)$, we can calculate all the other optical properties like reflectivity $R(\omega)$, refractive index $n(\omega)$, extinction coefficient $\kappa(\omega)$, absorption coefficient $\alpha(\omega)$ and optical conductivity $\sigma(\omega)$ [32]. The imaginary part of the dielectric constant. The optical properties of the material can be found by relation (1)

3.2.1. Imaginary part

The imaginary part is calculated theoretically using the following relation:

$$\varepsilon_2(\omega) = \left(\frac{4\pi^2 e^2}{m^2 \omega^2} \right) \sum_{i,j} \int i |M_{ij}|^2 f_i (1 - f_j) \delta(E_f - E_i - \omega) d^3K \quad (3)$$

where M is the dipole matrix; i and j are initial and final states respectively; f_i is the Fermi distribution function for the its state; E_i is the energy of electron in the ith state and ω is the frequency of the incident photon.

Figure 1 shows imaginary part of the dielectric constant of ZnO.

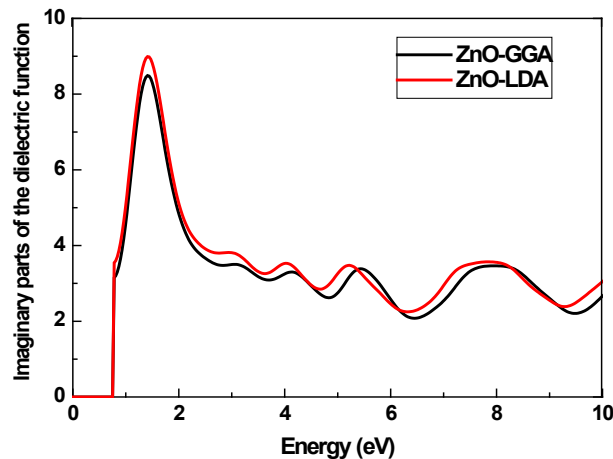


Fig. 1. Imaginary part of the dielectric constant of ZnO.

Figure 1 represents the changes in the values of the imaginary part of the dielectric constant in terms of energy. We note that the first peak of the maximum absorption intensity was recorded at the value 2 eV, which reaches a peak of 9. This results from the movement of electrons from the highest valence band to the lowest point in the conductivity band. Afterwards, a decreasing curve of changes in the values of the imaginary part is recorded in the range extending from (2.5 to 25) eV, until it reaches 0, thus the valence band is devoid of electrons.

3.2.2. Absorption coefficient

It is the phenomenon of spreading light inside the material due to its absorption of the incident light ray, given by the following relation:

$$\alpha(\omega) = \frac{\epsilon_2(\omega) \cdot \omega}{c \cdot n} \quad (4)$$

where ω is the frequency, c : the speed of light in vacuum, n : the refractive index. Fig. 2 represents the absorption coefficient of ZnO using GGA and LDA.

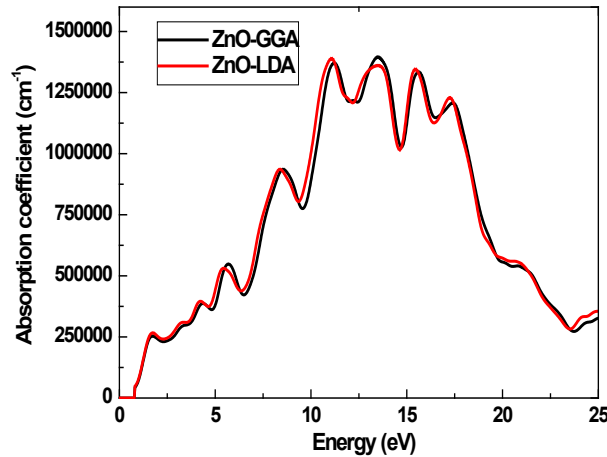


Fig. 2. The absorption coefficient of ZnO.

Figure 2 represents the changes of the absorption coefficient in terms of energy E_g (eV) using the two approximations (GGA, LDA), which seem almost identical. The curve can be divided into three areas:

a) Basic absorption area: Which is in the range between (0 to 0.68) eV, in which no values of absorption appear, but rather, rapid absorption occurs when the absorbed radiation energy is equal to the energy gap, representing the least energy difference between the highest level in the valence band and the lowest level in the conduction band, called E_g .

b) Minimum absorption area: Found in the two ranges going from (0.68 to 10) eV and (18 to 25) eV, which corresponds to the absorption values ranging from (0 to 7600) cm^{-1} , and (30000 to 50000) cm^{-1} respectively. This absorption is very weak, which makes it difficult for us to study the absorbency, as the electrons are moving from one level to another.

c) Maximum absorption area:

It is ranged between (10 to 18) eV, corresponding to the absorption values (75000 to 76000) cm^{-1} . This represents the maximum absorption intensity, that is, the electrons move from the valence band to the conduction band in the levels extending between them. This is noticeable from the maximum absorption intensity that is followed by three peaks at: 11 eV, 13 eV and 16 eV, corresponding to the absorbency intensities estimated at (1375000, 1375000 and 1370000) cm^{-1} respectively.

To conclude, the analysis of the above curve in the cases of using GGA and LDA show that ZnO is transparent in the visible area of the ranges from (0.68 to 10) eV and (18 to 25) eV. Besides, it is a good absorbent in the ultraviolet area within the range from (10 to 18) eV.

3.2.3. Extinction coefficient

The extinction coefficient k is the amount of energy, absorbed by the material electrons, of the incident light ray photons. This coefficient is given according to the following relation.

$$K(\omega) = \left[-\frac{\varepsilon_1(\omega)^{1/2}}{2} + \frac{\sqrt{\varepsilon_1^2(\omega) + \varepsilon_2^2(\omega)}}{2} \right]^{1/2} \quad (5)$$

Whereas: $\varepsilon_1(\omega)$: real part of the dielectric constant, $\varepsilon_2(\omega)$: the imaginary part of the dielectric constant. The figure (3) hereunder shows the changes of the extinction coefficient k of ZnO in terms of energy.

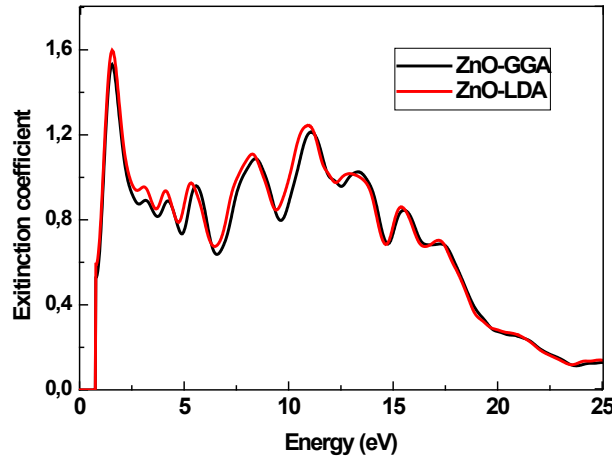


Fig. 3. Extinction coefficient K of ZnO.

Figure 3 represents the changes of the extinction coefficient in terms of energy in (eV) unit, using the approximations GGA and LDA. We note that in the range from (0 to 0.68) eV, no value of the extinction coefficient was recorded, due to its presence in the energy gap area, while in the range extending from (0.68 to 2) eV, we note that the extinction coefficient increases gradually along with the increase of energy and reaches its maximum at the basic absorption area. In the range (2 to 25) eV, this area witnessed a set of weak oscillations. It is recorded during which two peaks at 7.5 eV and 10.25 eV, corresponding to 0.11 and 1.2 respectively. This oscillation is due to the behaviour of light at the level of semiconductors [33].

3.2.4. Optical conductivity

It is defined as the increase in the number of carriers (electron holes), as a result of the incident light beam on the material, symbolized by: $\sigma(\omega)$, Figure 4 shows the optical conductivity results of ZnO using the GGA and LDA.

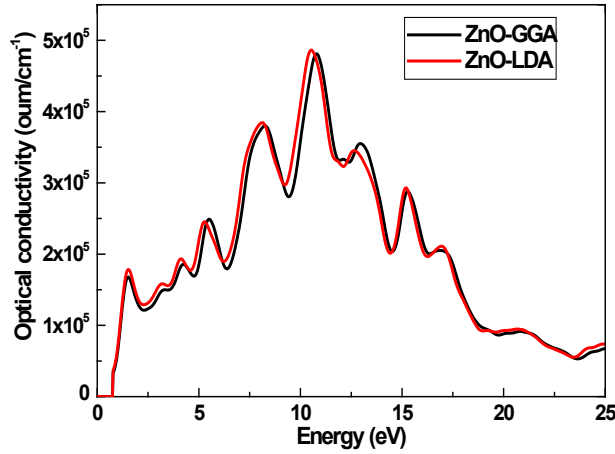


Fig. 4. Optical conductivity of ZnO.

Figure 4 represents the changes in the optical conductivity values in terms of energy in (eV) unit, by using both GGA and LDA. In general, the results of the optical conductivity values using both approximations show that they are very similar. We notice in the range extending from (0 to 0.68) eV that no value for the optical conductivity is recorded, because it exists in the energy gap area, while in the range extending from (0.68 to 12) eV, we see that the values of the optical conductivity are in a noticeable increase until they reach the peak at energy of 11eV, which corresponds to 490000 (oum/cm⁻¹). In the range (12 to 25) eV, there is a very large decrease of the value of the conductivity, i.e. (49000 to 50000) (oum/cm⁻¹). By analyzing the absorbency and optical conductivity curves, we concluded that the rheological shape of both is the same; this confirms the fact that ZnO is a semiconductor [34].

3.2.5. Reflectivity

The reflectivity R is defined as the ratio of the reflected light (ray) IR of the incident lightbeam with a given wavelength on a given surface, and the incident light (ray) IR.

$$R = \frac{(n-1)^2 + k^2}{(n+1)^2 + k^2} \quad (6)$$

where: n is the real part of the complex refractive index, k: is the imaginary part of the refractive index, When k=0 we find that:

$$R = \frac{(n-1)^2}{(n+1)^2} \quad (7)$$

When n=0, we find that R= 1. Fig. 5 represents the reflectivity curve of ZnO using the GGA and LDA.

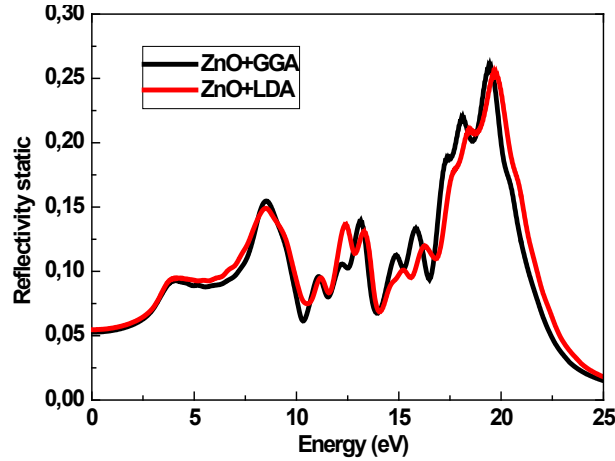


Fig. 5. The reflectivity of ZnO.

Fig. (5) represents the reflectivity curve $R(\omega)$ in terms of energy. It is noted that the reflectivity increases from the value 0.05 at energy 0 eV until it reaches the value 0.27 at energy 20 eV. Then, it decreases rapidly at higher energies. This means that ZnO behaves like a semiconductor [35].

3.2.6. Refractive index

Refraction is an optical property of a material with a refractive index that depends on the polarization and direction of light propagation. Refraction is measured as the difference between normal and abnormal refractive indices. The refractive index can be calculated by the following relation:

$$n(\omega) = \left[\frac{\epsilon_1(\omega)^{1/2}}{2} + \frac{\sqrt{\epsilon_1^2(\omega) + \epsilon_2^2 \epsilon_1(\omega)}}{2} \right]^{1/2} \quad (8)$$

Fig.6 shows the refractive index curve of ZnO using GGA and LDA.

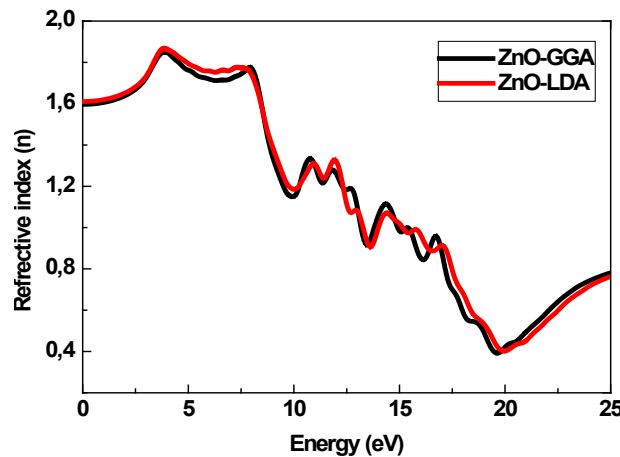


Fig. 6. Refractive index of ZnO.

Fig. 6 represents the curve of the refractive index $n(\omega)$ in terms of energy (eV), where the refraction is important only in the non-absorbed area, which is under the energy gap. The value of the static refractive index (n_0) of the compound ZnO is 1.6, then the refractive index $n(\omega)$

increases along with the increase of the energy of the incident photons, reaching the value of 1.9 at the energy 4eV. Some decreasing oscillations were observed in the refractive index curve by increasing the incident energy until it reaches the value of 19 eV, where the path of the decreasing curve changes to increase the value of the refractive index against the increase in the energy of the incident photons.

4. Conclusion

We have analysed both the structural and optical properties of the wurtzite phase ZnO using PP-LAPW method and the Siesta code. Besides, the exchange-correlation effects have been treated by GGA-PBE and LDA-CA approximations. The results of the structural study show a great consistency with the previously calculated theoretical values, and all the optical properties that were calculated, such as the imaginary part of the dielectric constant, the reflectivity $R(\omega)$, the refractive index $n(\omega)$, the extinction coefficient $k(\omega)$, the absorption coefficient $\alpha(\omega)$, and the optical conductivity $\sigma(\omega)$, confirmed the unique properties of ZnO that were shown by previous experimental results.

References

- [1] J. Serrano, A. H. Romero, F.J. Manjon, *et al.*, Phys. Rev. B. **69**.P. 094306 (2004); <https://doi.org/10.1103/PhysRevB.69.094306>
- [2] Y. Chen, H. Li, D. Huang *et al.*, Mater. Sci.Semicond. Process **148**. P.106807(2022); <https://doi.org/10.1016/j.mssp.2022.106807>
- [3] H.Wang, Y. Li, C.Wangetal., Sensors and Actuators B: Chemical. **339**. P. 129888 (2021); <https://doi.org/10.1016/j.snb.2021.129888>
- [4] M.A.Khan, N. Nayan, M. K.Ahmad *et al.*, Surf. Interfaces **21**. P.100649 (2020); <https://doi.org/10.1016/j.surfin.2020.100649>
- [5] M.Abdelfatah, H.Y.Salah, M.I.EL-Henaweyet *et al.*, J. Alloys Compd. **873**.P.159875(2021); <https://doi.org/10.1016/j.jallcom.2021.159875>
- [6] G.C.Zhou, L. Z.Sun, J.B.Wanget al., Phys. B: Condens. Matter. **403**. P. 2832-2837 (2008) <https://doi.org/10.1016/j.physb.2008.02.018>
- [7] C.H.Bates, W. B.White, R.Roy, Science 1962. **137**. P. 993 (1962); DOI: [10.1126/science.137.3534.993](https://doi.org/10.1126/science.137.3534.993)
- [8] K.Harun, N. A.Salleh, B.Deghfel, *et al.*, Results. Phys. **16**. P. 102829 (2020); <https://doi.org/10.1016/j.rinp.2019.102829>
- [9] E.Benrezgaa, A.Zoukel, B.Deghfel, *et al.*, Mater.Today. Commun. **31**.P.103306 (2022); <https://doi.org/10.1016/j.mtcomm.2022.103306>
- [10] R. John, S. Padmavathil, Cryst. struct. theoryappl. **05**.P. 24-41(2016); <http://dx.doi.org/10.4236/csta.2016.52003>
- [11] F. J. Kong, G.Jiang, Phys. B: Condens. Matter **404**. P. 2340-2344(2009); <http://dx.doi.org/10.1016/j.physb.2009.04.041>
- [12] Q.Wang, C.Zahou, W.Ju, *et al.*, Comput. Mater. Sci. **102**. P.196-201(2015); <https://doi.org/10.1016/j.commatsci.2015.02.035>
- [13] L. Zhao, P.F.Lu, Z.Y.Yu, *et al.*, First-principles study of electronic and optical properties in wurtzite $Zn_{1-x}Cu_xO$. *Chin. Phys. B*. **19**. P. 056104 (2010); <https://doi.org/10.1088/1674-1056/19/5/056104>
- [14] P.A.Rodnyi, I.V.Khodyuk, Opt.Spectrosc. **111**. P. 776-785(2011); <http://dx.doi.org/10.1134/S0030400X11120216>
- [15] G.Tse, Comput. Condens. Matter. **24**.e00525(2021); <https://doi.org/10.1016/j.cocom.2020.e00525>
- [16] R.A.Zargar, K. Kumar, Z. M.M.Mahmoud *et al.*, Phys. B: Condens. Matter **631**. P. 413614.(2022); <https://doi.org/10.1016/j.physb.2021.413614>

- [17] A.D.Becke, E.R. Johnson, J. Chem. Phys.**124**. P. 221101(2006);<https://doi.org/10.1063/1.2213970>
- [18] E.S. Huber, M. Hellstrom, M. Probst et al., Surf. Sci. **628**. P. 50-61(2014);
<https://doi.org/10.1016/j.susc.2014.05.001>
- [19] F.Oba, A.Togo, I.Tanaka et al., Phy. Rev. B **77**.P. 245202 (2008);
<https://doi.org/10.1103/PhysRevB.77.245202>
- [20] R.Farooq, T. Mahmood, A.W.Anwaret al., Superlattices Microstruct.**90**. P.165–169(2016);[doi: 10.1016/j.spmi.2015.12.017](https://doi.org/10.1016/j.spmi.2015.12.017).
- [21] M.K.,Yaakob, N.H. Hussin,M.F.M. Taib et al., Integr. Ferroelectr.**155**.P. 15-22 (2014);<https://doi.org/10.1080/10584587.2014.905086>
- [22] E. Kisi, M.M. Elcombe, Acta Cryst. **C45**. P.1867-1875(1989);
<https://doi.org/10.1107/S0108270189004269>
- [23] D. C. Reynolds D.C. Look, B. Jogai et al., Phys.Rev. B **60**. P. 2340-2344 (1999);<https://doi.org/10.1103/PhysRevB.60.2340>
- [24] Landolt-Börnstein, New Series, K. H. Hellwege (ed.), Group III: Crystal and Solid State Physics, Vol. 12: Magnetic and Other Properties of Oxides and Related Compounds, Part c: Hexagonal Ferrites. Special Lanthanide and Actinide Compounds. Springer-Verlag Berlin, Heidelberg, New York: 1982 <https://doi.org/10.1002/crat.2170181220>
- [25] G.Yao, G. Fan, F. Zhao, et al., Phys. B: Condens. Matter **407**. P. 3539-3542 (2012);
<https://doi.org/10.1016/j.physb.2012.05.019>
- [26] W. Jun, J.Hu,L.Shao et al., Mater.SciSemicond.process **29**. P. 245-249 (2015); [DOI: 10.1016/j.mssp.2014.03.050](https://doi.org/10.1016/j.mssp.2014.03.050)
- [27] A. A.Mohamad, M.S.Hassan,M.K..Yaakob et al., J. King saud.Univ-Eng Sci.**29**. P. 278-283(2017); <https://doi.org/10.1016/j.jksues.2015.08.002>
- [28] F.Decremps, F. Datchi, A. M. Saitta et al., Phys. Rev B. **68**. P.104101 (2003);<https://doi.org/10.1103/PhysRevB.68.104101>
- [29] H. Karzel, W. Potzel, M. Kofferlein et al., Phys.Rev. B **53**. P. 11425 (1996); <https://doi.org/10.1103/PhysRevB.53.11425>
- [30] N. V. Smith, Phys. Rev. B **3**. P.1862-1878 (1971); <https://doi.org/10.1103/PhysRevB.3.1862>
- [31] C. M.I.Okoye,J. Condens. Matter Phys.**15**. P. 5945-5958 (2003);<https://doi.org/10.1088/0953-8984/15/35/304>
- [32] J. Sun, H.T. Wang, J.L. He et al., Phys. Rev. B **71**.P. 125132(2005);
<https://doi.org/10.1103/PhysRevB.71.125132>
- [33] D. Allali, A. Bouhemadou, F. Zerarga et al., J. Nanoelectron. Optoelectron. **14**. P.1-8(2019);
[DOI: 10.1166/jno.2019.2552](https://doi.org/10.1166/jno.2019.2552)
- [34] Taira H., Shaima H., Solid State Commun. 2014. **177**. P. 61-64;
<https://doi.org/10.1016/j.ssc.2013.10.002>
- [35] B.Cakmak, T.Karacali, Z.Renet et al., Microelectron. Eng. **87**. P.2343-2347 (2010);
<https://doi.org/10.1016/j.mee.2010.04.004>